

A Study on Hydrogen Bonding in Controlled-Structure Benzoxazine Model Oligomers

*Ho-Dong Kim, Hatsuo Ishida**

Department of Macromolecular Science and Engineering, Case Western Reserve University, Cleveland, OH 44106, USA
E-mail: hxi3@cwru.edu

Summary: The synthesis procedure for controlled-structure benzoxazine model oligomers is described. To understand the complex hydrogen bonding structure, a series of benzoxazine model oligomers is characterized by nuclear magnetic resonance spectroscopy (NMR), Fourier transform infrared spectroscopy (FT-IR). The NMR resonances for model oligomers are newly assigned. The FT-IR spectra for model benzoxazine oligomers are carefully investigated both in crystalline and solution states. The distribution of hydrogen bonding species in benzoxazine model oligomers is quantitatively analyzed using FT-IR spectra. The cyclic conformations for the oligomers are also proposed.

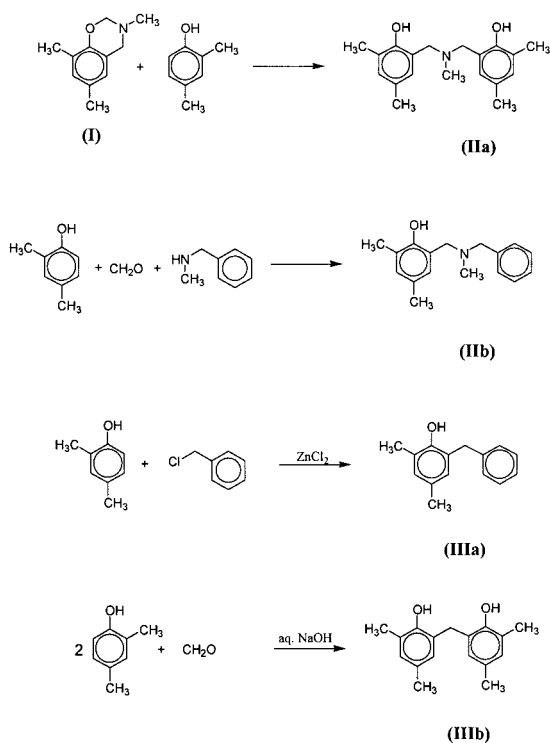
Keywords: benzoxazine; FT-IR; hydrogen bonding; model oligomers; NMR

Introduction

This study expands upon the previous work done on hydrogen bonding structure of benzoxazine model dimers^[1] which represent the typical polybenzoxazines. Polybenzoxazines are a new class of phenolic resins which have excellent mechanical and physical properties^[2–5] as well as ease of processing. Many studies^[6–11] have been done on the structures of traditional phenolic resins using model compounds because the typical instrumentation for polymeric materials cannot be applied to thermoset polymeric materials due to their intractable nature. However, most of the information from the studies for traditional phenolic resins cannot be applied to interpret the structure of polybenzoxazines due to the difference in the repeating unit. Although the phenolic resins have shown both intermolecular and intramolecular hydrogen bonding between hydroxyl groups, the hydrogen bonding structure in polybenzoxazine is much more complex due to the Mannich bridge structure.

Therefore, the need exists for understanding the structures of benzoxazine model compounds,

which allows experimental simulation and identification of the actual structure. Although a comprehensive characterization of the benzoxazine model dimer has already been accomplished in previous work by our research group,^[12-13] the analysis for the higher oligomers such as the model trimer and tetramer was incomplete due to the difficulties in obtaining highly purified compounds. The characterization of model oligomers, which have various chain lengths, can provide a better understanding of the structure-property relationships of the final polymer. Furthermore, a new conformational structure for benzoxazine oligomers based on the intramolecular hydrogen bond formation can be introduced. Therefore, the highly purified model compounds are synthesized in this paper and will be characterized. Also, the hydrogen bonded structure of the oligomers will be discussed.



Scheme 1. Synthesis of model dimers.

Experimental

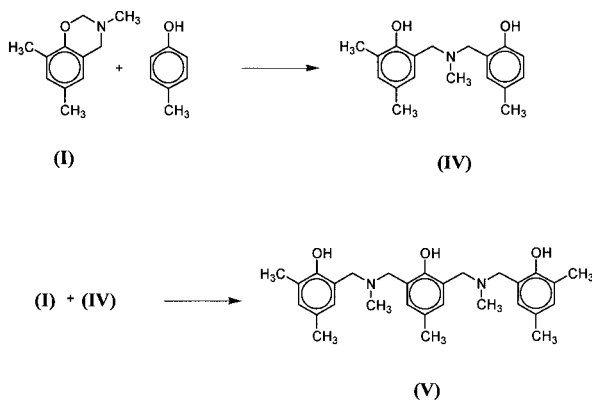
All chemicals were used as received. 2,4-Dimethylphenol (98%), *p*-cresol (99%), formaldehyde (37% in water), and methylamine (40% in water) were obtained from Aldrich Chemical Company.

Synthesis of N,N-bis(3,5-dimethyl-2-hydroxybenzyl)methylamine (IIa, Scheme 1, Methyl-dimer) and N-benzyl-N-(3,5-dimethyl-2-hydroxybenzyl)methylamine (IIb, Scheme 1, Asymmetric Methyl-dimer). Model dimers for polybenzoxazine were synthesized according to a previous study using 2,4-dimethylphenol, formaldehyde, methylamine, and N-methylbenzylamine.^[1]

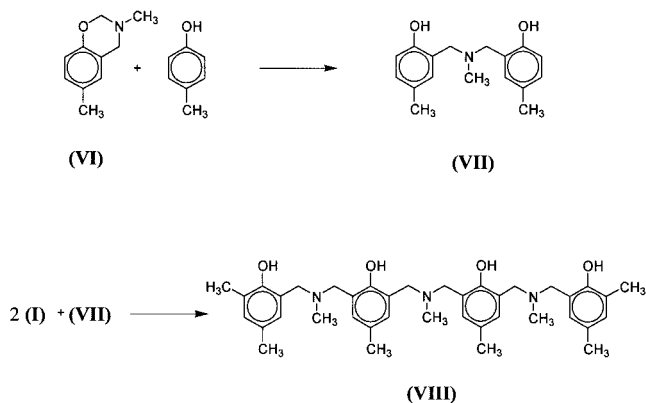
Synthesis of 2-benzyl-4,6-dimethylphenol (IIIa, Scheme 1, OH- π -dimer). OH- π -dimer was prepared by heating a mixture of 0.01 mole of 2,4-dimethylphenol, 0.01 mole of benzyl chloride, and 5 mg of zinc chloride at 95 °C for 3 hr.^[14]

Synthesis of 2,2'-methylene-4,4',6,6'-tetramethyldiphenol (IIIb, Scheme 1, Phenolic-dimer). One mole of 2,4-dimethylphenol and an excess of aqueous formaldehyde (2 mole) were refluxed in 1000 ml of 5% aqueous sodium hydroxide for 4 h. The dark brown mixture was cooled and neutralized with hydrochloric acid. The pale precipitate was collected by filtration, and recrystallized from n-hexane until a white crystal is obtained.^[15]

Synthesis of 2,6-Bis[N-(3,5-dimethyl-2-hydroxybenzyl)-N-methylamino-methyl]-*p*-cresol (V, Scheme 2, Methyl-trimer). The starting monomer, 3,4-dihydro-3,6,8-trimethyl-2H-1,3-benzoxazine I, was prepared by the procedure described by Dunkers and Ishida.^[13] To obtain the intermediate dimer IV, equimolar portions of the monomer I and *p*-cresol were heated at 80 °C for 12 h, and the resulting yellow product was recrystallized from n-hexane. This intermediate dimer IV was reacted again with an equimolar portion of the monomer I without reaction solvent at 80 °C for 48 h. The resulting yellow product was cooled and was subsequently purified by column chromatography with silica gel using hexane/acetone (20:1) as the eluent. White fine crystal. ¹H-NMR (200 MHz, CDCl₃, 298K) δ : 2.20, 2.21 (15H, Ar-CH₃), δ : 2.22 (6H, N-CH₃), 3.68 (8H, Ar-CH₂-N), and 6.70, 6.84, 6.86 (6H, Ar-H). ¹³C-NMR (50.1 MHz, CDCl₃, 298K) δ : 15.81, 20.27 (5C, Ar-C), 40.95 (2C, N-CH₃), 58.78, 59.59 (4C, Ar-C-N), and 122.14 ~ 154.05 (18C, Ar). Anal. found: C, 75.09; H, 8.30; N, 6.11. Calcd. for C₁₉H₂₅NO₂: C, 75.29; H, 8.28; N, 6.06.



Scheme 2. Synthesis of model trimer.



Scheme 3. Synthesis of model tetramer.

Synthesis of N,N-Bis{2-hydroxyl-5-methyl-3-[(N-3,5-dimethyl-2-hydroxyl-benzyl)-N-methylaminomethyl]}-methylaniline (VIII, Scheme 3, Methyl-tetramer). The model tetramer for polybenzoxazine was synthesized according to the following procedure using 2,4-dimethylphenol, *p*-cresol, formaldehyde, and methylamine. The starting monomer, 3,4-dihydro-3,6-dimethyl-2H-1,3-benzoxazine VI, was prepared by the procedure described by Dunkers and Ishida.^[13] The intermediate dimer VII was synthesized by heating equimolar portions of the

monomer VI and *p*-cresol at 80 °C for 12 h, and the resulting yellow product was recrystallized from *n*-hexane. The mixture of intermediate dimer VII and monomer I (1:2 mole ratio) was refluxed in chloroform for 48 h. After the reaction mixture was cooled to room temperature, chloroform was removed with a rotary evaporator, and the resulting yellow solid was subsequently purified by column chromatography with silica gel using hexane/acetone (20:1) as the eluent. White fine powder. ¹H-NMR (200 MHz, CDCl₃, 298K) δ: 2.19, 2.21 (18H, Ar-CH₃), δ: 2.23 (9H, N-CH₃), 3.63, 3.66 (12H, Ar-CH₂-N), and 6.66, 6.84, 6.86 (8H, Ar-H). ¹³C-NMR (50.1 MHz, CDCl₃, 298K) δ: 15.81, 20.27 (6C, Ar-C), 40.95 (3C, N-CH₃), 57.57, 58.38, 59.59 (6C, Ar-C-N), and 121.84 ~ 153.65 (24C, Ar). Anal. found: C, 74.66; H, 7.99; N, 6.84. Calcd. for C₁₉H₂₅NO₂: C, 74.85; H, 8.21; N, 6.71.

Instrumentation The purity of the monomers and dimers was examined using a Varian XL200 nuclear magnetic resonance spectrometer (¹H-NMR and ¹³C-NMR) and elemental analysis at M-H-W Laboratories. Deuterated chloroform and deuterated acetic acid were used as NMR solvents with 0.5 % tetramethylsilane as the internal standard. Coaddition of 256 transients yielded a good signal-to-noise ratio spectrum. Relaxation time (D1) of 10 seconds was used to obtain integration results.

Fourier transform infrared (FT-IR) spectra were obtained on a Bomem Michelson MB110 FT-IR spectrophotometer which was equipped with a liquid nitrogen cooled, mercury-cadmium-telluride (MCT) detector with a specific detectivity, D*, of 1x10¹⁰ cmHz^{1/2}W⁻¹. Coaddition of 128 scans was recorded at a resolution of 2 cm⁻¹ after 20 min purge with dry nitrogen. FT-IR spectra of the crystalline samples were taken as a thin powder layer between two KBr plates. The KBr pellet technique was not used in order to prevent water from interfering with the OH stretching region of interest. The solution spectra for the dimers in CCl₄ were obtained in a KRS-5 liquid cell at 298 K with a 0.5 mm thickness for 10 mM, 20 mM and 50 mM concentrations, and in a barium fluoride liquid cell with a 5 mm thickness for 1 mM and 5 mM concentrations. The spectrum of the liquid cell with spectrophotometric grade carbon tetrachloride (CCl₄) was subtracted from the solution spectra. Heavily overlapped bands in the hydroxyl stretching region of FT-IR spectrum from 2000 cm⁻¹ to 4000 cm⁻¹ were curve-resolved using a mixed Lorentzian-Gaussian function in GRAMS/32 (Galactic software). It was calculated until the least-squares curve-fitting converged. Molecular modeling was performed on a Power Macintosh G4 450 MHz using CONFORMER

2.0 (PrincetonSimulations) and CS Chem3D Pro 4.0 (CambridgeSoft®) which incorporates the weighted random walk Monte Carlo search algorithm^[16] with MM2 force field energy minimization and MOPAC energy minimization.

Results and Discussion

Synthesis of Methyl-trimer and Methyl-tetramer Since it is well known that Methyl-dimer can be synthesized by the ring opening reaction of benzoxazine monomer to the *o*-position of a corresponding phenol compound,^[13] the synthesis of Methyl-trimer and Methyl-tetramer was attempted by the same experimental procedure. However, while the reaction of monomer I with *o*-cresol gave a fairly good yield to form dimer IV, the reaction for Methyl-trimer V from monomer I and dimer IV ended with an extremely low yield. The reaction for Methyl-tetramer also showed a similar result. Considering the methylamine based benzoxazine monomer is very reactive to form Methyl-dimer,^[17-18] this result is highly unusual. A similar difficulty was already reported by Ishida and Krus^[19] and the obstacle for purification was also reported even in the well-designed bromination-debromination reaction for benzoxazine oligomers. Also, Imoto et al.^[20] reported that the intramolecular hydrogen bonding to form cyclic conformers is responsible for this behavior. However, since it can give great insight into the polybenzoxazine structure, a more detailed and accurate characterization of oligomers was carried out in a systematic manner despite the low yield of the desired oligomers.

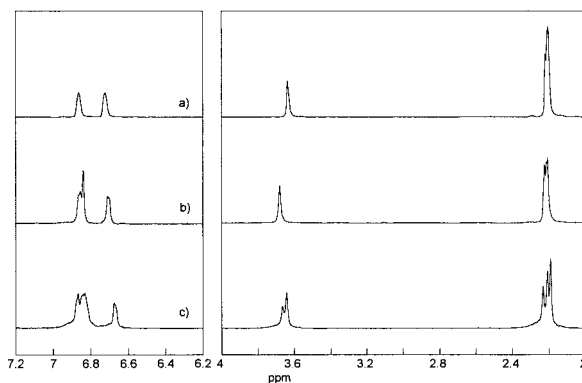
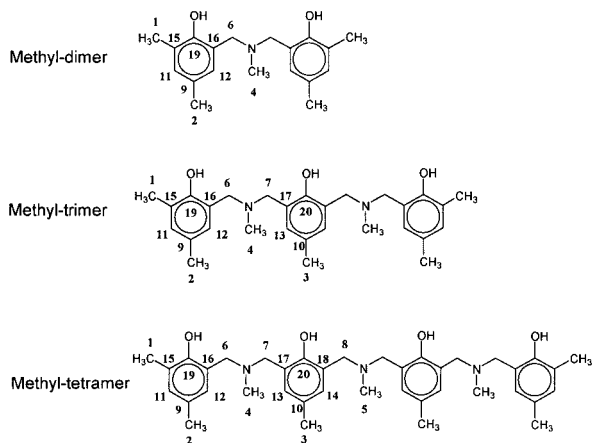


Figure 1. ¹H-NMR Spectra of a) Methyl-dimer, b) Methyl-trimer, and c) Methyl-tetramer in deuterated chloroform.

To investigate the molecular structure, ^1H -NMR and ^{13}C -NMR spectra in different deuterated solvents were obtained and summarized in Table 1. Using assignment of the ^1H NMR resonances in deuterated chloroform for Methyl-dimer reported by Dunkers and Ishida,^[13] the spectra of Methyl-trimer and Methyl-tetramer in deuterated chloroform are assigned. (Figure 1)

Table 1. ^1H -NMR and ^{13}C -NMR assignments for model benzoxazine oligomers.

Assignment	^1H in CDCl_3 (ppm)			^1H in CD_3COOD (ppm)			^{13}C in CDCl_3 (ppm)		
	Dimer	Trimer	Tetramer	Dimer	Trimer	Tetramer	Dimer	Trimer	Tetramer
C1	2.22	2.20	2.19	2.22	2.19	2.18	15.74	15.86	15.77
C2	2.22	2.20	2.19	2.22	2.22	2.21	20.41	20.40	20.40
C3	-	2.21	2.21	-	2.29	2.28	-	20.45	20.46
C4	2.24	2.22	2.23	2.79	2.82	2.79	41.06	40.90	40.99
C5	-	-	2.23	-	-	2.81	-	-	41.06
C6	3.66	3.68	3.64	4.14-4.52	4.12-4.49	4.11-4.46	59.25	58.69	57.50
C7	-	3.68	3.64	-	4.12-4.49	4.11-4.46	-	59.68	58.58
C8	-	-	3.66	-	-	4.11-4.46	-	-	59.77
C9	-	-	-	-	-	-	124.24	124.52	122.86
C10	-	-	-	-	-	-	-	127.74	124.31
C11	6.73	6.71	6.67	6.92	6.94	6.92	128.24	128.05	127.60
C12	6.89	6.86	6.87	7.00	7.00	6.99	130.84	130.14	129.92
C13	-	6.84	6.83	-	7.29	7.27	-	130.77	130.22
C14	-	-	6.84	-	-	7.28	-	-	130.55
C15	-	-	-	-	-	-	121.80	122.14	121.83
C16	-	-	-	-	-	-	121.80	122.65	122.78
C17	-	-	-	-	-	-	-	128.15	127.83
C18	-	-	-	-	-	-	-	-	127.83
C19	-	-	-	-	-	-	152.00	152.36	152.66
C20	-	-	-	-	-	-	-	153.91	153.65



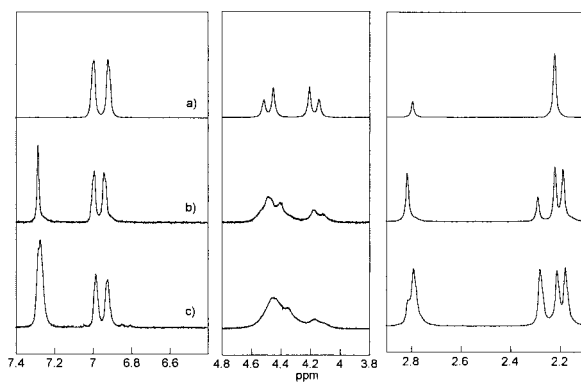


Figure 2. ^1H -NMR Spectra of a) Methyl-dimer, b) Methyl-trimer, and c) Methyl-tetramer in deuterated acetic acid.

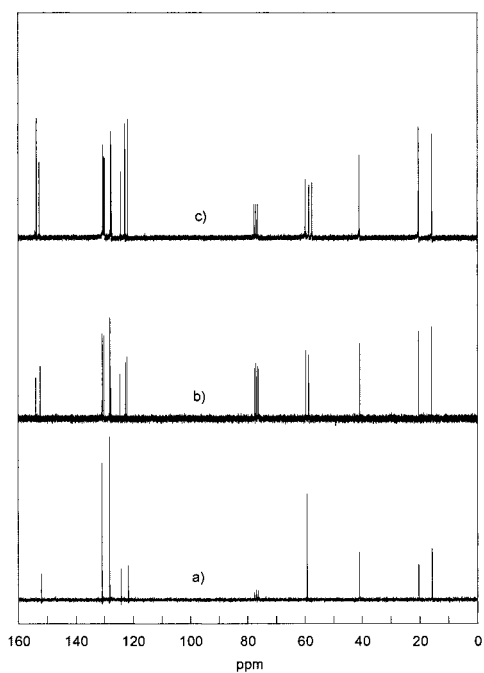


Figure 3. ^{13}C -NMR Spectra of a) Methyl-dimer, b) Methyl-trimer, and c) Methyl-tetramer in deuterated deuterated chloroform.

However, more accurate assignments can be obtained from the ^1H -NMR spectra in deuterated acetic acid as the solvent. Because the protons, which are adjacent to the nitrogen, can be deshielded due to the salt formation between the nitrogen atom and acetic acid, the chemical shifts of the adjacent protons are shifted downfield. These effects on the ^1H -NMR chemical shift of the model benzoxazine dimers were investigated in detail by Kim and Ishida^[3]. Therefore, using acetic acid as a NMR solvent, the resonance for aminomethyl protons is easily distinguished from the resonances for aromatic methyl protons. As shown in Figure 2, the resonances for the aromatic methyl protons in Methyl-trimer and Methyl-tetramer are well resolved from the resonance for the aminomethyl protons. Also, the resonances for aromatic methyl protons, which are not discernable in the spectrum of Methyl-dimer, are obviously distinguished. Therefore, the resonances at 2.19 ppm, 2.22 ppm and 2.29 ppm in Methyl-trimer are assigned to the protons 1, 2 and 3, respectively. The resonances for Methyl-tetramer are also assigned to the sequence and the integrals of the peaks support these assignments. Evidently, the resonance at 2.82 ppm in Methyl-trimer is assigned to the protons 4, and the resonances at 2.79 ppm and 2.81 ppm in Methyl-tetramer are assigned to the protons 4 and 5, respectively. The nonequivalence of aminomethyl protons in Methyl-tetramer is also confirmed by ^{13}C -NMR spectra which will be discussed later. The resonances for the methylene protons show the typical AB quartet^[3] spectra due to the salt formation and the typical line broadening of the spectra appeared with increased chain length.

The other important feature of ^1H -NMR in deuterated acetic acid is found in the region of aromatic protons. The resonances for aromatic protons, which are ambiguously assigned due to the overlapping of the peaks in the spectra with deuterated chloroform, are clearly acquired. Using the better resolved resonances and the integrals of the peaks, the resonances at 7.29 ppm in Methyl-trimer and at 7.27 ppm and 7.28 ppm in Methyl-tetramer are assigned to the aromatic protons 13 and 14. Additionally, these assignments for the spectra in deuterated acetic acid make the assignment for the spectra in deuterated chloroform more clear.

The ^{13}C -NMR spectra of the model oligomers shown in Figure 3 also contains many of the same peaks found in the spectra of the model dimer. However, the most important information for the oligomer structure is found from the methylene carbon resonances in Mannich base which are obtained from the highly purified Methyl-trimer and Methyl-tetramer. The methylene carbons in

Mannich bases exhibit a doublet for Methyl-trimer and a triplet for Methyl-tetramer centered around 59 ppm, whereas the Mannich bridge carbons of the model dimer showed only one resonance at 59.25 ppm. This implies that a magnetic non-equivalence exists among the methylene carbons in the benzoxazine model oligomers. Therefore, based on these resonances, the interpretation shown above seems more appropriate than previously explained.^[19]

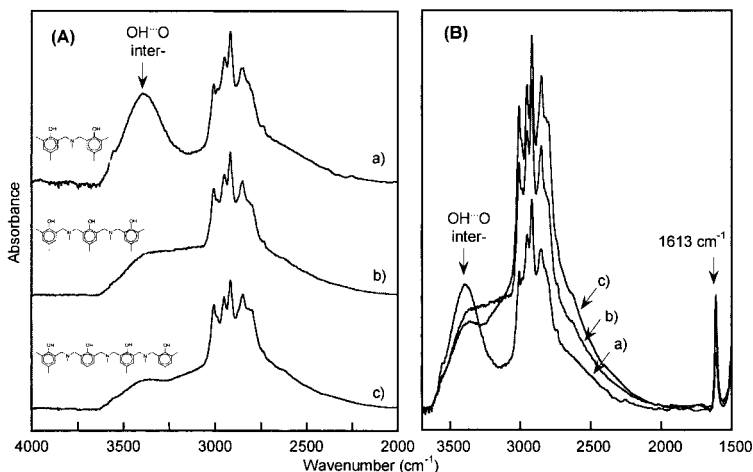


Figure 4. (A) Comparison of FT-IR spectra for a) Methyl-dimer, b) Methyl-trimer, and c) Methyl-tetramer in crystal state. (B) Intensity corrected by 8b vibrational band (benzene) at 1613 cm^{-1} .

FT-IR Spectra of Model Oligomers As shown in Figure 4A, the band around 3400 cm^{-1} , which represents the $\text{--OH}\cdots\text{O}$ intermolecular hydrogen bonding, decreases in intensity with the increased chain length. Since the hydroxyl group in benzoxazine model compounds forms very stable $\text{--OH}\cdots\text{N}$ intramolecular hydrogen bonding,^[1] the $\text{--OH}\cdots\text{O}$ intermolecular hydrogen bonding can be formed only between the hydroxyl groups which are not participating in the $\text{--OH}\cdots\text{N}$ intramolecular hydrogen bonding. Therefore, the band around 3400 cm^{-1} should represent the one $\text{--OH}\cdots\text{O}$ intermolecular hydrogen bonding in each molecule. If this explanation is valid, the intensity of the $\text{--OH}\cdots\text{O}$ intermolecular hydrogen bonding remains constant with respect to the internal reference, even though the unit length of model compounds is increased. This

explanation is well supported by the fact that the $\text{-OH}\cdots\text{O}$ intermolecular hydrogen bonding for each molecules have almost the same intensity, when the FT-IR spectra are normalized and compensated by benzene vibrational (8b) band at 1613 cm^{-1} ^[13] (Figure 4B). However, when Methyl-trimer and Methyl-tetramer are compared with Methyl-dimer, the situation is quite different. The fact that the $\text{-OH}\cdots\text{O}$ intermolecular hydrogen bonding in Methyl-trimer and Methyl-tetramer show lower intensity band (arrow mark in Figure 4B) than that in Methyl-dimer suggests that a hydrogen bonding structure is changed.

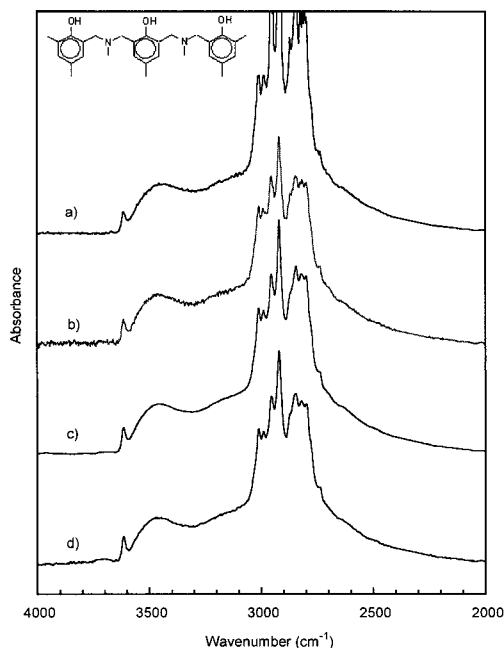
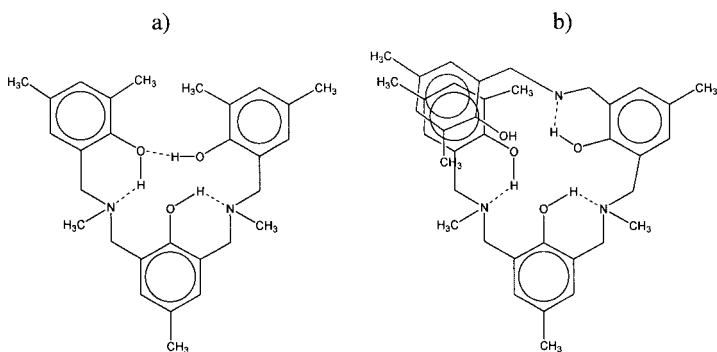


Figure 5. FT-IR spectra for Methyl-trimer in CCl_4 solution; a) 50 mM, b) 10 mM, c) 5 mM, and d) 1 mM concentrations.

Since the FT-IR frequencies for individual hydrogen bonding species in benzoxazine model dimers have been investigated in detail by Kim and Ishida,^[1,18] the band assignment for the each group will not be repeated in this paper. Taking into account that the structures of model trimer

and tetramer are very similar except for the total length, it is expected that the FT-IR spectra in CCl_4 will also show the similar trend. However, unexpectedly, a new band centered at 3461 cm^{-1} appears in the Methyl-trimer spectrum as shown in Figure 5. Since this band is not dependant on the concentration, it implies that the conformation of Methyl-trimer has the intramolecular association which does not appear in the Methyl-dimer spectrum. From the chemical structure of Methyl-trimer, a logically possible intramolecular association is $-\text{OH}\cdots\text{O}$ intramolecular hydrogen bonding. Since the $-\text{OH}\cdots\text{N}$ intramolecular hydrogen bonding in Methyl-dimer is very stable and the only dominant intramolecular interaction,^[1,18] the existence of $-\text{OH}\cdots\text{O}$ intramolecular hydrogen bonding is very unlikely. However, from the frequency of $-\text{OH}\cdots\text{O}$ intramolecular hydrogen bonding, which appears at 3461 cm^{-1} in the FT-IR spectrum of the diluted Phenolic-dimer (Figure 6), it can be assigned that the new band at 3461 cm^{-1} in Methyl-trimer spectrum is originated from $-\text{OH}\cdots\text{O}$ intramolecular hydrogen bonding. By introducing this new intramolecular hydrogen bond, which is an the ambiguously broad band in the FT-IR spectrum of the diluted Methyl-dimer and could not be understood very well in the previous paper,^[1] can now be explained. Therefore, to accommodate all hydrogen bonding species found in the FT-IR spectra, a pseudocyclic structure of Methyl-trimer is proposed in Scheme 4a. This cyclic structure based on intramolecular hydrogen bonding has been reported by Tobiason et. al.^[21-22] using molecular modeling of novolak oligomers and by Cairns and Eglinton^[23] using solution FT-IR for novolak dimers.



Scheme 4. Proposed structure of a) Methyl-trimer and b) Methyl-tetramer.

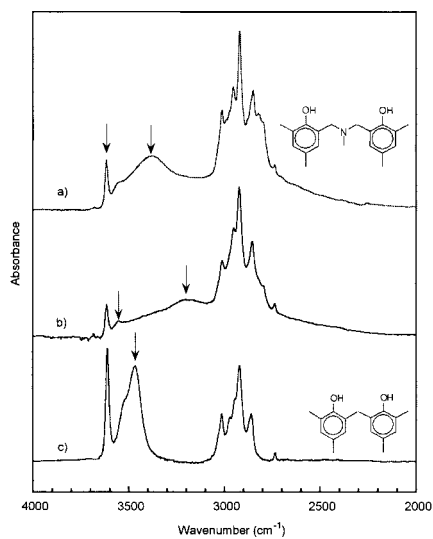


Figure 6. FT-IR spectra for dimers in CCl_4 solution; a) 50 mM Methyl-dimer, b) 1 mM Methyl-dimer, and c) 1 mM Phenolic-dimer.

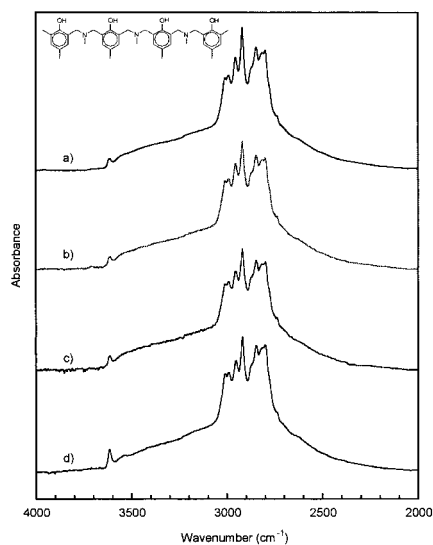


Figure 7. FT-IR spectra for Methyl-tetramer in CCl_4 solution; a) 20 mM, b) 10 mM, c) 5 mM, and d) 1 mM concentrations.

The spectra for Methyl-tetramer in CCl_4 solution also show a similar trend (Figure 7), even though the band for $-\text{OH}\cdots\text{O}$ intramolecular hydrogen bonding is broad and weak. The intensity decrease in this band can be understood as $-\text{OH}\cdots\text{O}$ intramolecular interaction between the end groups is weakening (Scheme 4b). This aspect will be discussed in the next section.

Quantitative Analysis of Hydrogen Bonding Species As discussed by Pimentel and McClellan,^[24] it is not easy to apply the quantitative analysis for the complex hydrogen bonded system since the behavior of compounds with intermolecular hydrogen bond is drastically different from that of intramolecular hydrogen bonded systems and the sensitivity of absolute intensity is very high. However, if the intensities of the band for each species are internally consistent, the fraction of each hydrogen bonding species can be determined. Also, simplified compounds which can simulate each hydrogen bonded species were used in order to obtain the absorption coefficients since the benzoxazine model compounds are consisted with at least 5 different hydrogen bond species.

The integrated intensity of curve-resolved bands were determined by GRAMS/32 software and the integrated absorption coefficients were obtained according to eq. (1).^[25-26]

$$S = \int A dv = \epsilon cl \quad (1)$$

where S is the area of absorption, A is the absorbance, ν is the frequency, ϵ is the apparent integrated molar absorption coefficient, c is the concentration of solution, and l is the path length of the cell.

As shown in Figure 8a, the apparent integrated molar absorption coefficient of free hydroxyl group (ϵ_{free}) is estimated by the diluted phenol in CCl_4 . The use of phenol as the model compound for the free OH band is justified as the free OH stretching frequency of phenol is within several wavenumbers of all the corresponding bands of the compounds studied. The FT-IR spectra of concentrated phenol solutions (Figure 8b) which consisted of two bands (free $-\text{OH}$ group and intermolecular hydrogen bond) is resolved into each band by GRAMS software. Then, the concentration of free $-\text{OH}$ groups (c_{free}) is calculated by eq. (2). Using eq. (1) and c_{inter} , the apparent integrated molar absorption coefficient of intermolecular hydrogen bonded $-\text{OH}$ (ϵ_{inter}) is obtained.

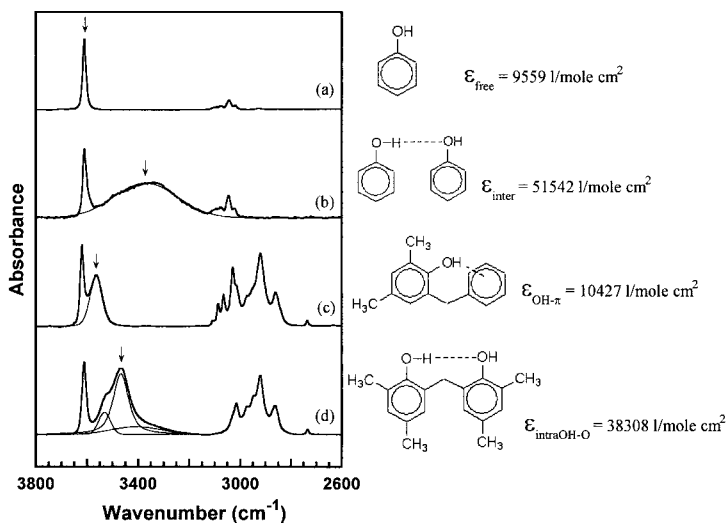


Figure 8. Curve-resolved FTIR spectra of each hydrogen bonding species for model compounds solution in CCl_4 : a) 3 mM of phenol, b) 250 mM of phenol, c) 5 mM of OH-p-dimer, and d) 5 mM of Phenolic-dimer.

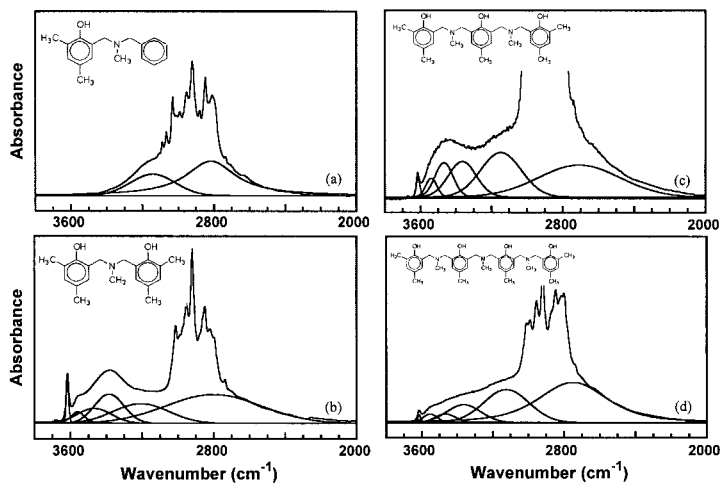


Figure 9. Curve-resolved FTIR spectra of benzoxazine model compounds in 50 mM CCl_4 solutions: a) Asymmetric Methyl-dimer, b) Methyl-dimer, c) Methyl-trimer, and d) Methyl-tetramer.

$$c_{free} = A / (\epsilon_{free} \times l) \quad (2)$$

$$c_{inter} = c_o - c_{free} \quad \text{where } c_o = \text{total concentration of -OH groups} \quad (3)$$

The apparent integrated molar absorption coefficient of OH- π intramolecular hydrogen bonded -OH ($\epsilon_{OH-\pi}$) can be estimated by the similar method using the FT-IR spectra for diluted OH- π -dimer in CCl_4 which shows two bands for free -OH group and OH- π intramolecular (Figure 8c). Also, the apparent integrated molar absorption coefficient of OH-O intramolecular hydrogen bonded -OH ($\epsilon_{intraOH-O}$) can be calculated from the spectra of Phenolic-dimer in CCl_4 (Figure 8d).

After the curve-resolving of FT-IR spectra for benzoxazine model compounds (Figure 9), the distribution of hydrogen bonded species in the model oligomers can be calculated using the ϵ values of each hydrogen bonded species and eq. (4) - (6).

$$c_* = A / (\epsilon_* \times l) \quad * : \text{free, inter, OH-}\pi, \text{ and intraOH-O} \quad (4)$$

$$c_{intraOH-N} = c_o - (c_{free} + c_{inter} + c_{OH-\pi} + c_{intraOH-O}) \quad (5)$$

$$\text{Fractions of each group} = c_* / c_o \quad (6)$$

It is shown in Table 2 that the hydrogen bonded species in the proposed molecular structures correspond well in the calculated distribution of hydrogen bonds. Especially, the fractions for OH-N intramolecular hydrogen bond are fell in the range of theoretically acceptable values within the experimental error. (Theoretical fractions for OH-N intramolecular hydrogen bond in asymmetric Methyl-dimer, Methyl-dimer, Methyl-trimer, and Methyl-tetramer are 1.00, 0.50, 0.66, and 0.75, respectively, for the proposed structure.) Also, the weakening of OH-O intramolecular hydrogen bond in Methyl-tetramer is well demonstrated in the small fraction value of 0.02.

Although it is well known that the generation of a satisfactory molecular model for polybenzoxazine is very difficult due to the presence of complex hydrogen bonding interaction,^[27-28] the general molecular modeling by MM2 and MOPAC for the small benzoxazine model oligomers can give us a good insight for the hydrogen bonding structure when

it is combined with the FT-IR result. Thus, in the cyclic structure of trimer as proposed in Scheme 4, the hydroxyl group which is not participating in $\text{--OH}\cdots\text{N}$ intramolecular hydrogen bonding occupies a favorable position to form $\text{--OH}\cdots\text{O}$ intramolecular hydrogen bonding. This proposed cyclic structure is supported by the molecular modeling results schematically shown in Figure 10a and consistent with the result proposed by Dunkers *et. al.*^[12] using the X-ray crystal structure of Methyl-dimer. On the other hand, the energy minimized structure for Methyl-tetramer starts showing the overlapping of chain ends as shown in Figure 10b. From this structure, it can be deduced that the diminishing of the band for $\text{--OH}\cdots\text{O}$ intramolecular hydrogen bonding in Methyl-tetramer is related to the spatial location of the hydroxyl group which does not form $\text{--OH}\cdots\text{N}$ intramolecular hydrogen bonding. A more rigorous quantum mechanical calculation of the oligomer structure is underway and will be reported elsewhere. While it is not for model oligomers of interest in this paper, rigorous molecular modeling of polybenzoxazine have been reported in the literatures.^[27-30]

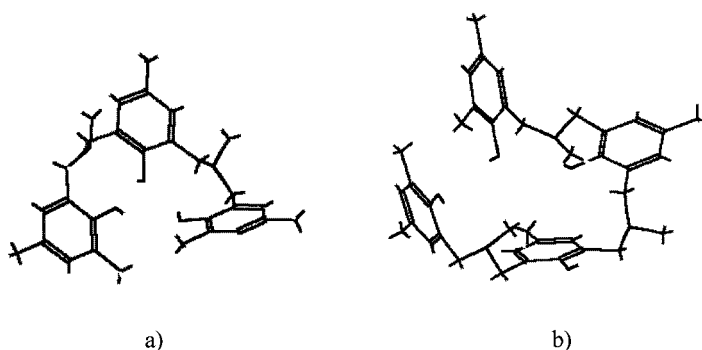


Figure 10. Energy minimized structure of a) Methyl-trimer and b) Methyl-tetramer.

Table 2. Distribution of hydrogen bonding species in benzoxazine model compounds in 50 mM CCl_4 solutions.

	Free OH 3615 cm^{-1}	OH- π intraHB 3559 cm^{-1}	OH-O intraHB 3467 cm^{-1}	OH-N intraHB $\sim 3000 \text{ cm}^{-1}$	OH-O interHB 3364 cm^{-1}
Asym. Methyl-dimer	-	-	-	1.00	-
Methyl-dimer	0.09	0.14	0.11	0.53	0.13
Methyl-trimer	0.04	0.11	0.09	0.67	0.10
Methyl-tetramer	0.01	0.04	0.02	0.88	0.05

Conclusion

Utilizing ^1H -NMR, ^{13}C -NMR, and FT-IR, the in-depth characterization for benzoxazine model oligomers has been made. The band for $-\text{OH}\cdots\text{O}$ intramolecular hydrogen bonding in benzoxazine model oligomers was newly assigned. Furthermore, it has been proposed that model oligomers can form a pseudocyclic structure based on the stable $-\text{OH}\cdots\text{N}$ intramolecular hydrogen bonding and $-\text{OH}\cdots\text{O}$ intramolecular hydrogen bonding. From the quantitative analysis of hydrogen bonding species in benzoxazine model oligomers, the distribution of the hydrogen bonding species has been discussed. With these findings, a deeper understanding for the structure of a new class of phenolic resin, polybenzoxazine, has been made and the possibility of helical structure formation in the longer chain benzoxazine oligomers has been predicted.

- [1] H. D. Kim, H. Ishida, *J. Phy. Chem. A* **2002**, *106*, 3271.
- [2] H. Ishida, H. Y. Low, *Macromolecules* **1997**, *30*, 1099.
- [3] H. D. Kim, H. Ishida, *J. Appl. Polym. Sci.* **2001**, *79*, 1207.
- [4] H. Ishida, D. J. Allen, *J. Polym. Sci., Polym. Phys.* **1996**, *34*, 1019.
- [5] H. Ishida, Y. Rodriguez, *Polymer* **1995**, *36*, 3151.
- [6] G. Casiraghi, M. Cornia, G. Sartori, G. Casnati, V. Bocchi, G. D. Andreetti, *Makromol. Chem.* **1982**, *183*, 2611.
- [7] G. Casiraghi, M. Cornia, G. Ricci, G. Balduzzi, G. Casnati, G. D. Andreetti, *Makromol. Chem.* **1983**, *184*, 1363.
- [8] G. Casiraghi, M. Cornia, G. Ricci, G. Casnati, G. D. Andreetti, L. Zetta, *Macromolecules* **1984**, *17*, 19.
- [9] E. Paulus, V. C. Paulus, *Makromol. Chem.* **1984**, *185*, 1921.
- [10] H. C. Paulus, K. Eberle, V. Bohmer, M. Grossmann, *Makromol. Chem.* **1975**, *176*, 3295.
- [11] L. Zetta, G. Casiraghi, M. Cornia, R. Kaptein, *Macromolecules* **1985**, *19*, 1622.
- [12] J. Dunkers, A. Zarate, H. Ishida, *J. Phys. Chem.* **1996**, *100*, 13514.
- [13] J. Dunkers, H. Ishida, *Spectrochim. Acta.* **1995**, *51A*, No. 5, 855.
- [14] A. Padwa, D. Dehm, T. Oine, G. A. Lee, *J. Am. Chem. Soc.* **1975**, *97*:7, 1837.
- [15] T. Dargaville, P. J. de Bruyn, A. S. C. Lim, M. G. Looney, A. C. Potter, D. H. Solomon, X. Zhang, *J. Polym. Sci., Polym. Chem. Ed.* **1997**, *35*, 1389.
- [16] G. Chang, W. C. Guida, W. C. Still, *J. Am. Chem. Soc.* **1989**, *111*, 4379.
- [17] W. J. Burke, J. L. Bishop, E. L. M. Glennie, W. N. Bauer, *J. Org. Chem.* **1965**, *Oct.*, 3423.
- [18] H. D. Kim, H. Ishida, *Macromolecules* **2002**, *submitted*.
- [19] H. Ishida, C. M. Krus, *Macromolecules* **1998**, *31*, 2409.
- [20] M. Imoto, I. Ijichi, C. Tanaka, M. Kinoshita, *Makromol. Chem.* **1968**, *113*, 117.
- [21] F. Tobiason, G. Cain, J. Anderson, *J. Polym. Sci., Polym. Chem. Ed.* **1978**, *16*, 275.
- [22] F. Tobiason, *J. Polym. Sci., Polym. Chem. Ed.* **1975**, *17*, 949.
- [23] T. Cairns, G. Eglinton, *J. Chem. Soc.* **1965**, 5906.
- [24] G. C. Pimentel, A. L. McClellan, "The Hydrogen Bond", W. H. Freeman and Company, London 1960, p.95.
- [25] C. M. Huggins, G. C. Pimentel, *J. Phy. Chem.* **1956**, *60*, 1615.
- [26] T. Tanaka, T. Yokoyama, Y. Yamaguchi, *J. Polym. Sci., Part A-1* **1968**, *6*, 2137.
- [27] W. K. Kim, W. L. Mattice, *Comput. Theor. Polym. Sci.* **1998**, *8*, 339.
- [28] W. K. Kim, W. L. Mattice, *Comput. Theor. Polym. Sci.* **1998**, *8*, 353.
- [29] W. K. Kim, W. L. Mattice, *Langmuir* **1998**, *14*, 6588.
- [30] W. K. Kim, W. L. Mattice, *Macromolecules* **1998**, *31*, 9337.